Finite element computation of turbulent compressible flows based on the k — ε model and SUPG stabilization

Bijan Mohammadi

Institut national de recherche en informatique et automatique
Domaine de Voluceau
BP 105
78153 Le Chesnay

RÉSUMÉ. *On utilise une technique d'éléments finis stabilisés Petrov-Galerkin pour la résolution des équations de Navier-Stokes et de k — ε. La comparaison avec des solutions analytiques et des données expérimentales montre que cette technique est une bonne alternative pour le calcul d'écoulements turbulents autour de configurations complexes. En particulier, la simplicité de la formulation ainsi que la simplicité d'une généralisation au 3D rendent cette approche d'autant plus attrayante.*

ABSTRACT. *The conservative Navier-Stokes and the k — ε equations are solved using a stabilized Streamline Petrov-Galerkin technique. The stabilization techniques employed are described and several numerical examples are reported. Comparison with analytical or experimental data for these cases shows that this technique may be a good alternative for computing complexe configurations of turbulent compressible flows. Specially this approach seems to be interesting because the simplicity of its formulation and also a possible easy extension to three dimensional configurations.*

MOTS-CLÉS : *stabilisation, SUPG, équations de Navier-Stokes, turbulence, modèle k — ε, approche bi-couche.*

KEY WORDS : *SUPG stabilization, Navier-Stokes equations, turbulence, k — ε, two-equation model, two-layer approach.*

Les figures et schémas explicatifs sont réunis en fin d'article.

Revue européenne des éléments finis. Volume 2 - n° 1/1993, pages 27 à 46

1. Introduction

The SUPG (streamline-upwind/Petrov-Galerkin) stabilization for compressible flows was first introduced, in the context of inviscid flows, in a 1982 NASA report by Tezduyar and Hughes [TEZ 82]. Since then, the SUPG formulation was successfully applied to inviscid and viscous flows based on both the conservation and entropy variables formulations [HUG 84, MAL 85, HUG 86a, HUG 86b, HUG 86c, BAE 91, BEA 92, ALI 92a, ALI92b]. It was shown, based on a set of test problems, by Le Beau and Tezduyar [BEA 91] and Le Beau et al [BEA 92] that, the SUPG formulation based on the conservation variables, supplemented with a shock capturing term, yields solutions which are not only just as good as but also barely distinguishable from those obtained with the entropy variables [MAL 85, HUG 86a, HUG 86b, HUG 86c]. The SUPG stabilization based on the conservation variables was also successfully applied, by Aliabadi and Tezduyar [ALI 92b] to viscous flows involving moving boundaries and interfaces.

In this article, we extend the SUPG formulation of viscous compressible flows based on the conservation variables [ALI 92a] to turbulent compressible flows with the $k-\varepsilon$ model [LAU 72]. The $k-\varepsilon$ model we use is an extension to compressible flows of its incompressible version [MOH 90, CAR 91, MOH 91a]. It is however well known that the $k-\varepsilon$ model is not valid in the vicinity of solid boundaries. Therefore, to avoid near-wall difficulties we use the two-layer approach developped by Mohammadi in [MOH 91a, MOH 91b]. This technique consists of using the $k-\varepsilon$ model only in the high Reynolds regions. On the other hand, in the low Reynolds regions a one-equation model is used. This technique is more complicated than a simple wall laws technique but more practical than a low Reynolds two-equation model. Our experience shows that the solutions obtained by this approach are less mesh dependent than those issued from low Reynolds two-equation model computations. This is because the turbulent quantities (especially ε) have very large gradients in the sublayer and then require considerably more grid points to be accurately computed.

Moreover, these techniques have other interesting features. For instance, both of the SUPG and the two-layer techniques are easy to generalize to three dimensional cases and also easy to implement on massively parallele architectures [BEH 92].

In section 2, we describe the compressible Navier-Stokes and the $k-\varepsilon$ equations. Sections 3 and 4 are devoted to the description of the numerical methods and stabilization techniques. In section 5, four numerical examples from turbulent flows are presented. More precisely, we first validate the solver on the classical case of the flow over a flat plate. Then three complex configurations involving separation and compressibility effects are treated. In the first one we consider the flow over a cylinder and the second and the third cases consist of the flow around the NACA 0012 airfoil at two different angles of attack and Mach number.

2. Governing Equations

Let $U = (\rho, \rho u_1, \rho u_2, \rho e, \rho k, \rho \varepsilon)$ be the vector of conservation variables. We consider the Reynolds averaged Navier-Stokes equations and the $k - \varepsilon$ eddy-viscosity model in conservation form:

$$\frac{\partial U}{\partial t} + \frac{\partial F_1(U)}{\partial x_1} + \frac{\partial F_2(U)}{\partial x_2} = \frac{\partial E_1(U)}{\partial x_1} + \frac{\partial E_2(U)}{\partial x_2} + S(U) \qquad [1]$$

with

$$F_1(U) = \begin{pmatrix} \rho u_1 \\ \rho u_1^2 + p \\ \rho u_1 u_2 \\ (\rho e + p) u_1 \\ \rho u_1 k \\ \rho u_1 \varepsilon \end{pmatrix}, \quad F_2(U) = \begin{pmatrix} \rho u_2 \\ \rho u_2 u_1 \\ \rho u_2^2 + p \\ (\rho e + p) u_2 \\ \rho u_2 k \\ \rho u_2 \varepsilon \end{pmatrix}, \qquad [2]$$

$$E_1(U) = \begin{pmatrix} 0 \\ \tau_{11} \\ \tau_{12} \\ \kappa_{tot} \dfrac{\partial i}{\partial x_1} + u_1 \tau_{11} + u_2 \tau_{12} \\ (\mu + \mu_t) \dfrac{\partial k}{\partial x_1} \\ (\mu + \dfrac{\mu_t}{\sigma_\varepsilon}) \dfrac{\partial \varepsilon}{\partial x_1} \end{pmatrix}, \quad E_2(U) = \begin{pmatrix} 0 \\ \tau_{21} \\ \tau_{22} \\ \kappa_{tot} \dfrac{\partial i}{\partial x_2} + u_1 \tau_{12} + u_2 \tau_{22} \\ (\mu + \mu_t) \dfrac{\partial k}{\partial x_2} \\ (\mu + \dfrac{\mu_t}{\sigma_\varepsilon}) \dfrac{\partial \varepsilon}{\partial x_2} \end{pmatrix} \qquad [3]$$

and

$$S(U) = \begin{pmatrix} 0 \\ 0 \\ 0 \\ 0 \\ S_k \\ S_\varepsilon \end{pmatrix} \qquad [4]$$

which contains the RHS of the turbulent equations. The viscous stress tensor components are defined as:

$$\tau_{11} = \mu_{tot}[2\frac{\partial u_1}{\partial x_1} - \frac{2}{3}(\nabla . u)], \qquad [5]$$

$$\tau_{12} = \mu_{tot}[\frac{\partial u_1}{\partial x_2} + \frac{\partial u_2}{\partial x_1}], \qquad [6]$$

$$\tau_{22} = \mu_{tot}[2\frac{\partial u_2}{\partial x_2} - \frac{2}{3}(\nabla . u)], \qquad [7]$$

where

$$p = (\gamma - 1)\rho i, \qquad [8]$$

$$e = i + \frac{1}{2}|u|^2 + k, \qquad [9]$$

$$\mu_{tot} = \mu + \mu_t, \qquad [10]$$

$$\kappa_{tot} = \mu\frac{\gamma}{Pr} + \mu_t\frac{\gamma}{Pr_t} \qquad [11]$$

with

$$\gamma = 1.4, Pr = 0.72. \qquad [12]$$

Moreover, we have two turbulent modelling constants $Pr_t = 0.9$ and $\sigma_\varepsilon = 1.3$. Here μ is the viscosity of the fluid given by the Sutherland law's, κ_{tot} is the total thermal conductivity, Pr and Pr_t are respectively the laminar and turbulent Prandtl numbers and S_k and S_ε are defined as:

In high-Reynolds number regions

$$S_k = \frac{\mu_t}{2}|\nabla u + \nabla u^t|^2 - \rho\varepsilon, \qquad [13]$$

$$S_\varepsilon = \frac{c_1\rho k}{2}|\nabla u + \nabla u^t|^2 - c_2\rho\frac{\varepsilon^2}{k}. \qquad [14]$$

The eddy viscosity is given by

$$\mu_t = c_\mu\rho\frac{k^2}{\varepsilon} \qquad [15]$$

where $c_1 = 0.129, c_2 = 1.92$ and $c_\mu = 0.09$ are modelling constants.

In low-Reynolds number regions

$$S_k = \frac{\mu_t}{2}|\nabla u + \nabla u^t|^2 - \rho\varepsilon, \qquad [16]$$

$$S_\varepsilon = 0. \qquad [17]$$

In this region, ε is defined from k by the following expression:

$$\varepsilon = \frac{k^{\frac{3}{2}}}{l_\varepsilon} \qquad [18]$$

and

$$\mu_t = c_\mu\rho\sqrt{k}l_\mu. \qquad [19]$$

l_μ and l_ε are two length scales containing the damping effects in the vicinity of the wall:

$$l_\mu = \kappa c_\mu^{-3/4} y(1 - exp(\frac{-y^+}{c})), \qquad [20]$$

$$l_\epsilon = \kappa c_\mu^{-3/4} y (1 - exp(-\frac{y^+}{2\kappa c_\mu^{-3/4}})) \qquad [21]$$

where $y^+ = \sqrt{k} y \rho / \mu$ is a local Reynolds number based on the distance to the wall and $c = 70$ and $\kappa = 0.45$ are two modelling constants. This two-layer approach is the generalization to compressible configurations of the technique introduced in [PA 88]. It has already been widely validated in [MOH 91a].

Matching conditions

The previous regions are defined through two conditions. A first condition based on the level of turbulence in the flow and a second one based on geometrical considerations. The level of turbulence is defined through y^+. A point is considered to be in the high-Reynolds number region if y^+ is big, otherwise it is considered to be in the low-Reynolds region. For our computation the frontier is set at $y^+ = 200$. As Patel [PA 88], we found that changes around this position slightly affect the results. From a computational point of view, to define y^+, we need for each point in the mesh, its normal distance to the wall: y. So, we compute the minimum distance between them and the wall-nodes and we use of this quantity instead y. Our experience shows that despite this is not exact, it is sufficient and the method is not greatly affected by this operation. Another remark is on the conveniency of the method because we don't need the friction at the wall to compute y^+.
Now concerning the geometrical condition: consider an external flow, usually the flow is laminar in regions outside boundary layers or wakes and the previous condition defines such a region to be a low-Reynolds number region. But, it is clear that for these regions the $k - \varepsilon$ model is more suitable. Therefore, we ignore the first condition if the point is far from the wall. To give an idea, in the case of the flow around an airfoil of chord L, the limit is set at $L/10$.

Initial and boundary conditions

Let Γ denotes the boundary of the computational domain Ω which is around (or adjacent to) a solid body B. We need to associate with (1) a set of initial and boundary conditions.
The flow is considered to be uniform at the inflow boundary:

$$\rho = \rho_\infty, \quad u = u_\infty, \quad T = T_\infty, \quad k = k_\infty, \quad \varepsilon = \varepsilon_\infty. \qquad [22]$$

On the solid boundary Γ_B we assume no-slip condition for u and homogenous Dirichlet condition for k, and either the adiabaticity or a specified temperature:

$$u = 0, \quad T = T_w \quad or \quad \frac{\partial T}{\partial n} = 0, \quad k = 0. \qquad [23]$$

Specifying ε at the wall is not necessary. Indeed, in the low-Reynolds number regions we compute ε by (18) to specify its boundary condition in the high-Reynolds number regions. Therefore, no boundary condition is necessary for ε at the wall. However, (18) degenerates at the wall. We simply avoid computing ε at the wall. The initial condition can be a uniform state

$$\rho(x,0)=\rho_\infty, \quad u(x,0)=u_\infty, \quad T(x,0)=T_\infty, \quad k(x,0)=k_\infty, \quad \varepsilon(x,0)=\varepsilon_\infty. \qquad [24]$$

Quasi-linearized system

For numerical implementation, we will consider the quasi-linear form of (1). For $i,j=1,2$, we have:

$$\frac{\partial U}{\partial t}+A_i\frac{\partial U}{\partial x_i}-\frac{\partial}{\partial x_i}(K_{ij}\frac{\partial U}{\partial x_j})=S(U) \qquad [25]$$

where

$$A_i=\frac{\partial F_i}{\partial U} \quad and \quad K_{ij}\frac{\partial U}{\partial x_j}=N_i.$$

Associated with the system (25), we assume we have an appropriate set of boundary and initial conditions.

3. The Finite element formulation

Let Ω^h be a finite element discretization of Ω into elements T_e with $e=1,..,nel$. We define the finite element interpolation function spaces S^h and V^h using P^1 elements for the trial solutions and weighting functions, respectively. These function spaces are selected with the Dirichlet boundary conditions in mind, as subsets of $[H^1(\Omega^h)]^6$, where $H^1(\Omega^h)$ represents the finite dimensional function space over Ω^h. The SUPG finite element formulation can be written as follows: find $U^h\in S^h$ such that $\forall\Phi^h\in V^h$

$$\int_{\Omega^h}\Phi^h(\frac{U^h_{n+1}-U^h_n}{\Delta t}+(A_i)^h_n\frac{\partial U^h_{n+1}}{\partial x_i}+S^-(U^h_n)U^h_{n+1})dx \qquad [26]$$

$$+\int_{\Omega^h}\frac{\partial\Phi^h}{\partial x_i}((K_{ij})^h_n\frac{\partial U^h_{n+1}}{\partial x_j})dx \qquad [27]$$

$$+\sum_{e=1}^{nel}\int_{T_e}\tau(A^T_k)^h_n\frac{\partial\Phi^h}{\partial x_k}(\frac{\partial U^h_{n+1}}{\partial t}+(A_i)^h_n\frac{\partial U^h_{n+1}}{\partial x_i}-\frac{\partial}{\partial x_i}((K_{ij})^h_n\frac{\partial U^h_{n+1}}{\partial x_j})+S^-(U^h_n)U^h_{n+1})dx \qquad [28]$$

$$+\sum_{e=1}^{nel}\int_{T_e}\delta\frac{\partial\Phi^h}{\partial x_i}\frac{\partial U^h_{n+1}}{\partial x_i}dx \qquad [29]$$

$$= \int_{\Omega^h} \Phi^h S^+(U_n^h) U_n^h dx + \sum_{e=1}^{nel} \int_{T_e} \tau (A_i^T)_n^h \frac{\partial \Phi^h}{\partial x_i} S^+(U_n^h) U_n^h dx \qquad [30]$$

where (26) and (27) represent the Galerkin part of the formulation, (28) the SUPG stabilization term, (29) the discontinuity capturing operator and (30) contains the contribution of the positive part of the right hand side. In this scheme, the right hand sides of the $k-\varepsilon$ model are treated semi-implicitly. More precisely, we have writen that

$$S = (S^+)_n^h U_n^h - (S^-)_n^h U_{n+1}^h \qquad [31]$$

where S^+ and S^- are diagonal matrix defined by:

$$(S^+)^h = Diag(0,0,0,0,\frac{S_5^+}{U_5},\frac{S_6^+}{U_6}) \quad and \quad (S^-)^h = Diag(0,0,0,0,\frac{S_5^-}{U_5},\frac{S_6^-}{U_6}) \qquad [32]$$

with S_5^+, S_5^- (resp. S_6^+, S_6^-) the positive and negative part of S_k (resp. S_ε). This splitting of the right hand side in positive and negative parts enforces the stability of the scheme and the positivity of k and ε [MOH 90].

The implementation of the previous scheme is done in term of increment of U ($\delta U = U_{n+1}^h - U_n^h$). In other words, at each iteration we have to solve

$$M\delta U = b. \qquad [33]$$

This implicit system of equations is preconditionned by the 6×6 block-diagonal part of M and is solved by a linear GMRES approach [SAA 89, SHA 90].

4. The SUPG and shock-capturing operators

In this section, we describe the SUPG and shock capturing operators used in the stabilized formulation (26)-(30).

The SUPG operator τ

The SUPG operator τ used in this formulation is based on the one developped by Aliabadi et al [ALI 92b] for viscous flows.

$$\tau = \frac{max(\alpha h_i\,|\beta_i|)}{c + |u.\beta|} \quad for \quad i = 1,2 \qquad [34]$$

where h_i the element lenght in the x_i direction, α a parameter controling the stability and accuracy of the scheme ($\alpha = 0.5$ in the present), c is the local speed of sound, $u = (u_1, u_2)$ and $\beta = (\beta_1, \beta_2)$ is defined by:

$$\beta = \frac{\nabla ||U||^2_{A_0^{-1}}}{||\nabla ||U||^2_{A_0^{-1}}||_2}. \qquad [35]$$

The shock capturing operator δ

The shock capturing operator δ is defined by:

$$\delta = diag[\delta_{NS}, \delta_{NS}, \delta_{NS}, \delta_{NS}, \delta_k, \delta_\varepsilon]. \qquad [36]$$

In (36), δ_{NS} is the shock capturing operator used for the Navier-Stokes part of the conservation variables which is derived from the shock capturing operator proposed for entropy variables [HUG 86c] by reverse transformation[BEA 91]:

$$\delta_{NS} = \left(\frac{A_i \frac{\partial U}{\partial x_i} . \tilde{A}_0^{-1} . A_j \frac{\partial U}{\partial x_j}}{\frac{\partial \xi_l}{\partial x_j} \frac{\partial U}{\partial x_j} . \tilde{A}_0^{-1} . \frac{\partial \xi_l}{\partial x_k} \frac{\partial U}{\partial x_k}} \right)^{1/2} \qquad [37]$$

where $\tilde{A}_0^{-1}$ is the jacobian of the transformation from the conservation to entropy variables.

On the other hand, δ_k and δ_ε are defined as:

$$\delta_k = \frac{||A_i(5,j) \frac{\partial U}{\partial x_i}(j)||_2}{||\frac{\partial \xi_l}{\partial x_j} \frac{\partial \rho k}{\partial x_j}||_2} \quad and \quad \delta_\varepsilon = \frac{||A_i(6,j) \frac{\partial U}{\partial x_i}(j)||_2}{||\frac{\partial \xi_l}{\partial x_j} \frac{\partial \rho \varepsilon}{\partial x_j}||_2}. \qquad [38]$$

Overall optimization

This section is devoted to the description of some of the techniques we use to optimize the numerical diffusion introduced above. A first optimization can be done by remarking that in regions where the solution is smooth the numerical viscosity introduced by the SUPG operator is sufficient and that on the other hand, the numerical viscosity introduced by the discontinuity capturing operator is dominant in shock regions. Therefore, to enforce the consistency of the scheme, we choose the SUPG operator by:

$$\tau = Max(0, \tau - \delta\Delta). \qquad [39]$$

where

$$\Delta = \frac{1}{(c + |u.\beta|)^2}. \qquad [40]$$

Another optimization of the SUPG operator consists of removing the numerical viscosity where the physical (sum of the turbulent and laminar) one dominates. For this, we rescale τ by the following function:

$$f(Pe) = 1 \quad if \quad Pe > 3 \quad and \quad f(Pe) = \frac{Pe}{3} \quad elsewhere \qquad [41]$$

where Pe is the mesh Peclet number.

5. Numerical examples

In this section we present some numerical results illustrating the ability of the finite element Navier-Stokes solver for computing compressible turbulent flows. We first present results for the classical case of the flow over a flat plat. The second case consists of the flow over a cylinder and in the two last cases we treat the flow around a NACA 0012 at two different incidences and Mach numbers. For all these cases, the convergence to the steady state solution was deemed to have occured when the global error based on the maximum difference between the values of all the variables in two successive iterations dropped by 4 orders of magnitude.

Flow over a flat plate

The first problem presented is a turbulent flow over a flat plate at $M_\infty = 0.5$ and $Re_{\infty/m} = 3.2 \times 10^6$. The mesh used for this case contains 3570 nodes. The first point is placed at $10^{-5}m$. Figure 1 shows the velocity profile and figure 2 the skin friction coefficient. The computed horizontal velocity and skin friction coefficient are compared with the theoretical $\frac{1}{7}$ power law and $(0.0375Re(x)^{-1/6})$ respectively. In both cases, the agreement with analytical solutions is quite good. As we have computed the flow up to the wall, the power law profile does not match the computed velocity profile in the near-wall region. For this computation we make the assumption that the transition from laminar to turbulent is done between $x = 0.12m$ and $x = 0.15m$. For this reason, we multiply the eddy viscosity by a function varying from zero to one through this zone. This explain the fast variation of the skin friction coefficient in this area.

Flow past a cylinder

The second problem studied consists of the flow past a circular cylinder in the super-critical Reynolds number range. The free stream Mach number is $M_\infty = 0.3$ and the Reynolds number $Re_{\infty/m} = 1.8 \times 10^6$. As we are looking for the steady state solution, we consider the flow past only half a cylinder. The cylinder is centered in $x = 0, y = 0$ and its diameter is two meters. The experimental data[ACH 68] show that the boundary layer changes without any intermediate state from laminar to turbulent. The transition point is located at about $x = -0.27m$. Therefore, in the laminar part of the boundary layer (for $x \leq -0.27m$) the eddy viscosity is set to zero. For this case we use a polar grid extending to 6 diameters away from the cylinder and having 121×101 nodes. The first grid point is located at $y = 10^{-5}m$. On the cylinder, no-slip boundary condition is used for u and k. On the center line, symmetry boundary condition is assumed for the velocity and homogenous Neumann boundary condition for the other quantities. Dirichlet boundary condition is used for all of the variables

on the first quarter of the external boundary (for $x \leq 0$):

$$\rho = 1, \quad u = 1, \quad v = 0, \quad T = T_\infty, \quad k = k_\infty \quad \varepsilon = \varepsilon_\infty$$

with $k_\infty = \varepsilon_\infty = 10^{-4}$. The pressure coefficient ($Cp = 2(p - p_\infty)/(\rho_\infty u_\infty^2)$) on the cylinder has been compared with experimental data [ACH 68] in Figure 3. As expected [MAJ 85, MOH 91a] the base pressure is over estimated specially in the separated region. Figure 4 shows respectively a partial view of the mesh and the iso Mach and the turbulent kinetic energy contours. This case shows however the robustness of the method.

Flow past a NACA 0012

Now we treat two configurations of transonic flows around NACA 0012 airfoil from the Viscous Transonic Airfoil Workshop [HOL 87] held at the AIAA 25th Aerospace Sciences Meeting at Reno, Nevada in January 87. For both cases the chord is one meter. Experimental data for the pressure coefficient on the airfoil surface are available[HAR 81]. The meshes used in both cases have the same number of nodal points and elements (8062 nodes and 7876 elements). The first point is located at arround $10^{-4}m$ from the body.

In the first case the free stream Mach and Reynolds numbers are $M_\infty = 0.7, Re_\infty = 9 \times 10^6$ and the angle of attack is 1.49 degrees. For this case the flow is attached and supersonic near the leading edge upper surface. Figure 5 shows the finite element mesh and its close-up view. The computed pressure coefficient is compared to the experimental data in Figure 6. Iso Mach, k and ε contours are shown in Figure 8. This computation has been done without taking into account the transition from laminar to tubulent.

For the second case the free stream Mach and Reynolds numbers are $M_\infty = 0.55, Re_\infty = 9 \times 10^6$ and the angle of attack is 8.34 degrees. This is a complex configuration for the following reasons: a supersonic bubble is well forward on the airfoil upper surface, the flow is slightly separated at the foot of the shock and the angle of attack is about one degree below the maximum lift value. The computed pressure coefficient is compared to the experimental data in Figure 7. The agreement is quite good except for the upper surface region near the leading edge. It seems that this is due to the fact that this computation has been done without taking into account the transition from laminar to tubulent. The maximum Mach number in the supersonic region is 1.06. Iso Mach, k and ε contours are shown in Figure 9. As for the flow past the cylinder, the scheme seems to be dissipative near the minimum pressure location. We have tried to refine the mesh near the body to remove as much as possible the artificial viscosity but soon we have encountred stability problems.

6. Summary and Concluding Remarks

An implicit finite element method for solving the compressible Navier-Stokes and $k-\varepsilon$ equations has been presented. A two-layer technique has been used to avoid near-wall difficulties. Numerical results illustrate the development and validation of the solver. Our experience shows that this SUPG technique is more sensitive to the presence of highly streched elements in the mesh than a Characteristic-Galerkin or a Finite Volume-Galerkin method [MOH 90, CAR 91, MOH 91a, MOH 91b]. Typically, it is recommended to avoid aspect ratio of more than 500. Such elements are often needed in high Reynolds number situations to accurately capture the boundary layers when the flow is computed up to the wall. Therefore, a wall law's technique should avoid this problem. Furthermore, the simplicity of the formulation makes this stabilized finite element approach easy to extend to three dimensional configurations. However, in [CHA 92], Mallet and al present several computations of turbulent flows on highly streched meshes using a Galerkin Least Square solver based on entropy variables. Therefore, more investigations are necessary to see why our formulation based on conservation variables fails at this point.

Acknowledgements

The author would like to thank professor Tayfun E. Tezduyar and the members of his research team at the University of Minnesota for their contributions to this work.

This research was partially sponsored by NASA-Johnson Space Center under grant NAG 9-449 and by NSF under grant MSM-8796352. Partial support for this work has also come from the Army Research Office contract number DAAL03-89-C-0038 with the Army High Performance Computing Research Center at the University of Minnesota.

7. References

[ACH 68] ACHENBACH E., *"Distribution of Local Pressure and Skin-Friction Around a Cicrular Cylinder in a Cross-Flow up to Re* $= 5.10^6$*"*, Journal of Fluid Mechanics, Vol. 34, pp. 625-639, 1968.

[ALI 92a] ALIABADI S. K., RAY S. E., TEZDUYAR T. E. *"SUPG Finite Element Computation of Viscous Compressible Flows based on the Conservation and Entropy Variables Formulations"*, University of Minnesota Supercomputer Institut preprint 92/136.

[ALI 92b] ALIABADI S. K., TEZDUYAR T. E. *"Space-Time Finite Element Computation of Compressible Flows Involving Moving Boundaries and Interfaces"*, AHPCRC report, in preparation.

[BEA 91] LE BEAU G. J., TEZDUYAR T. E., *"Finite Element Computation of Compressible Flows with the SUPG Formulation"*, Advances in Finite Element Analysis in Fluid Dynamics, Eds. M.N. Dhaubhadel, M.S. Engelman and J.N. Reddy, FED-Vol.123, ASME, New York, 1991.

[BEA 92] LE MBEAU G. L., RAY S. E., ALIABADI S. K., TEZDUYAR T. E. *"SUPG Finite Element Computation of Inviscid Compressible Flows based on the Conservation and Entropy Variables Formulations"*, University of Minnesota Supercomputer Institut Preprint 92/26.

[BEH 92] BEHR M., JOHNSON A., KENNEDY J., MITTAL S., TEZDUYAR T., *Computation of Incompressible Flows with Implicit Finite Element Implementations on the Connection Machine*, AHPCRC preprint 92-045.

[CAR 91] CARDOT B., MOHAMMADI B., PIRONNEAU O., *"A Few Tools for the Implementation of Turbulence Models in Navier-Stokes Solvers"*. Incompressible CFD-Trends and Advances, Eds Max D. Gunzburger and R.A.Nicolaides, Cambridge University Press, pp. 25-39, 1991.

[CHA 92] CHALOT F., JOHAN Z., MALLET M., RAVACHOL M., ROGE G., *Development of a finite element Navier Stokes solver with applications to turbulence and hypersonic flows*, AIAA paper 92-0670.

[HAR 81] HARRIS C. D. *"Two-Dimensional Aerodynamic Characteristics of the NACA 0012 in the Langley 8-Foot Transonic Pressure Tunnel"*, NASA report TM 81927, 1981.

[HOL 87] HOLST T. L. *"Viscous Transonic Airfoil Workshop Compendium of Results"* AIAA paper 87-1460.

[HUG 84] HUGHES T.J.R. and TEZDUYAR T.E.*"Finite Element Methods for First-Order Hyperbolic Systems with particular Emphasis on the Compressible Euler Equations"*, Computer Methods in Applied Mechanics and Engineering, num. 45, pp. 217-284, 1984.

[HUG 86a] HUGHES T. J. R., FRANCA L.P., MALLET M.," *A New Finite Element Formulation for Computational Fluid Dynamics: I. Symmetric Forms of the Compressible Euler and Navier-Stokes Equations and the Second Law of Thermodynamics"*, Computer Methods in Applied Mechanics and Engineering, num. 54, pp. 223-234, 1986.

[HUG 86b] HUGHES T. J. R., MALLET M.," *A New Finite Element Formulation for Computational Fluid Dynamics: III. The Generalized Streamline Operator for Multidimensional Advective-Diffusive Systems"*, Computer Methods in Applied Mechanics and Engineering, num. 58, pp. 305-328, 1986.

[HUG 86c] HUGHES T. J. R., MALLET M.," *A New Finite Element Formulation for Computational Fluid Dynamics: IV. Discontinuity Capturing Operator for Multi-Dimensional Advective-Diffusive Systems"*, Computer Methods in Applied Mechanics and Engineering, num. 58, pp. 329-339, 1986.

[LAU 72] LAUNDER B.E., SPALDING D.B., *"Mathematical Models of Turbulence"*, Academic Press, 1972.

[MAJ 85] MAJUMDAR S., RODI W., *"Numerical Calculations of Turbulent*

Flow Past Circular Cylinders", Proc. on 3rd symp. on numerical and physical aspects of aerodynamic flows, Long Beach, Ca., pp. 3,13-3,25, Springer-Verlag Ed, Jan. 1985.

[MAL 85] MALLET M.," *A Finite Element Method for Computational Fluid Dynamics"*, Ph. D. Thesis, Department of Civil Engineering, Stanford University, 1985.

[MOH 90] MOHAMMADI B., *"A Stable Algorithm for the $k-\varepsilon$ Model for Compressible Flows"*, 1990, INRIA report num. 1355.

[MOH 91a] MOHAMMADI B., *"Complex Turbulent Flows Computation with a Two-Layer Approach"* , Int. J. Num. Meth. Fluids, Vol. 15, 747-771, 1992.

[MOH 91b] MOHAMMADI B. *"Etude du Modèle $k-\varepsilon$ de la Turbulence pour les Ecoulements Compressibles"*, Ph.D. Thesis, University of Paris VI, 1991.

[PA 88] Patel V.C., Chen H.C., *Near-wall turbulence models for complex flows including separation*, AIAA Journal vol. 29, No. 6, June 1988.

[SAA 86] SAAD Y. and SCHULTZ M., *"GMRES: A Generalized Minimum Residual Algorithm for Solving Nonsymmetric Linear Systems"*, SIAM Journal of Scientific and Statistical Computing, Vol. 7, No. 3, pp. 856-869, 1986.

[SHA 90] SHAKIB F., Finite Element Analysis of the Compressible Euler and Navier Stokes Equations, Ph.D. Thesis, Stanford Univ. 1988.

[TEZ 82] TEZDUYAR T. E. and HUGHES T.J.R,*"Development of Time-accurate Finite Element Techniques for First-Order Hyperbolic Systems with-Particular Emphasis on the Compressible Euler Equations"*, report prepared under NASA-Ames university consortium, Interchange No. NCA2-OR745-104, 1982.

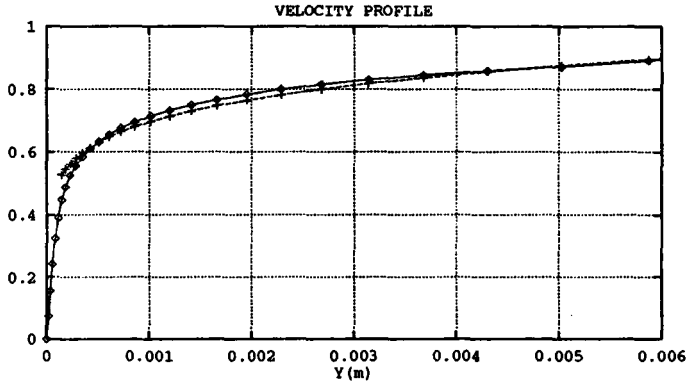

Figure 1. *Flow over a flat plate : velocity profile (+ theoretical)*

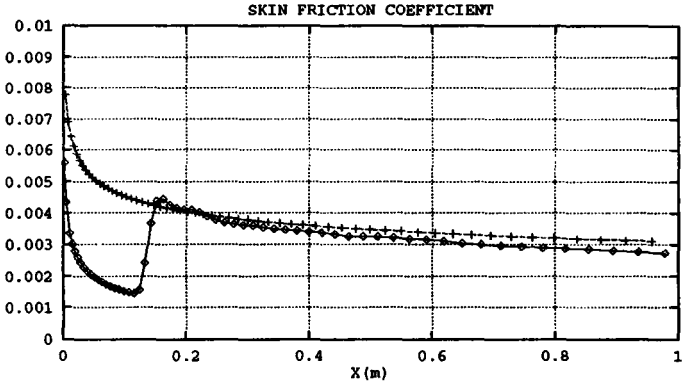

Figure 2. *Flow over a flat plate : skin friction coefficient (+ theoretical)*

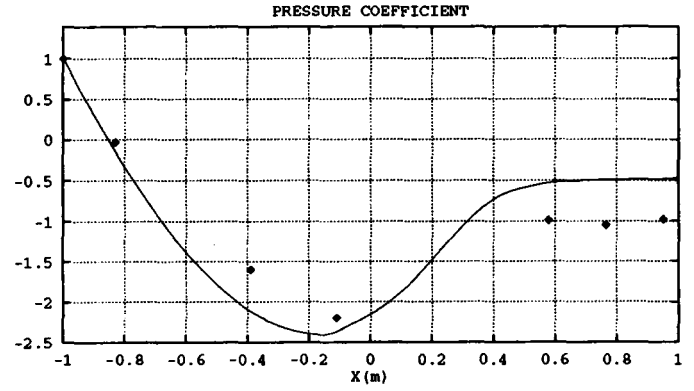

Figure 3. *Flow past a cylinder : C_p on the cylinder surface ($\oplus$ from [ACH 68])*

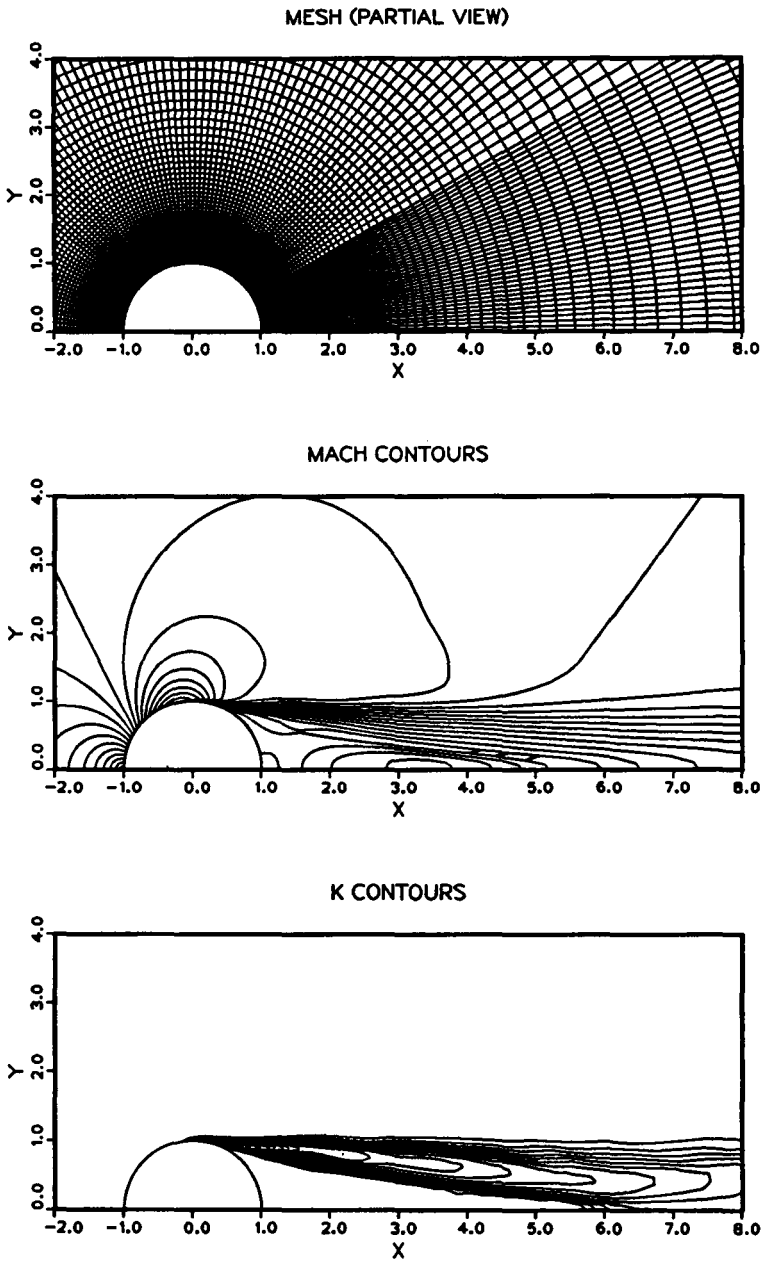

Figure 4. *Flow past a cylinder : partial view of the mesh, iso Mach number and k contours*

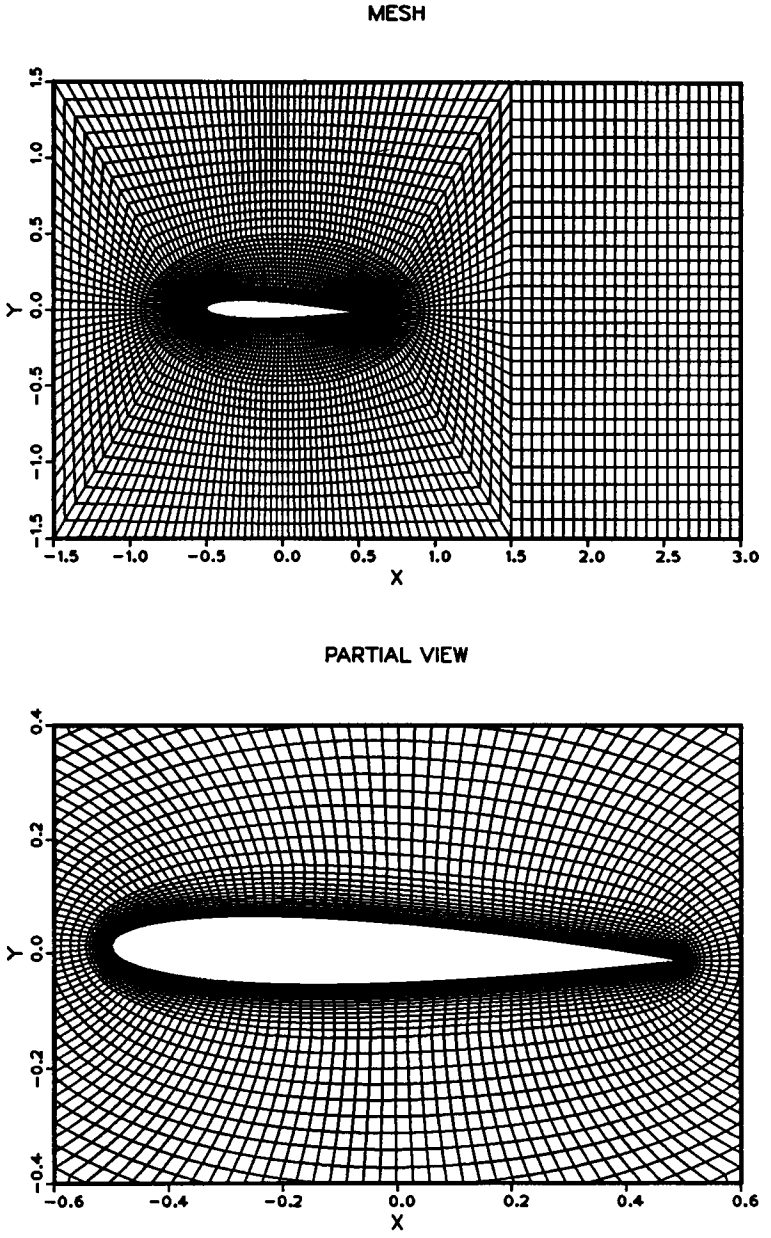

Figure 5. *Flow past a NACA 0012 : finite element mesh and the close-up view of the mesh*

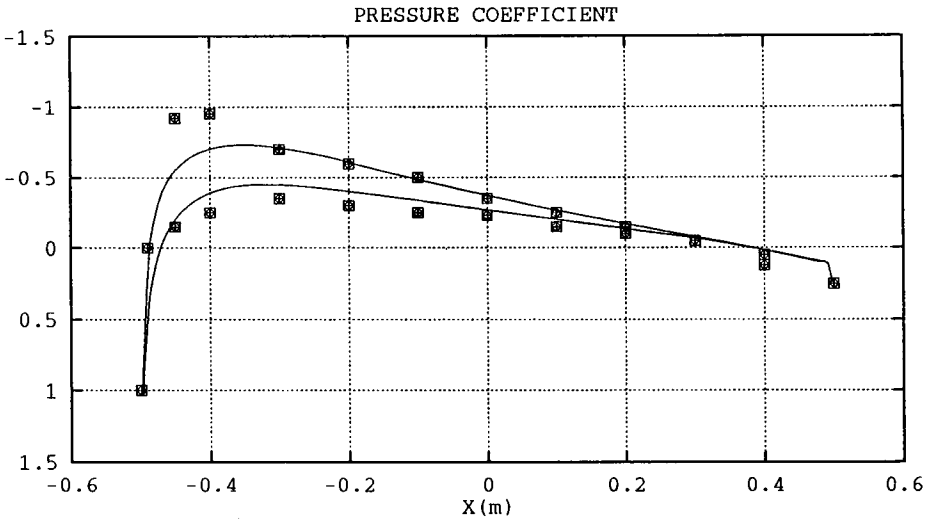

Figure 6. *Flow past a NACA 0012 at Mach 0.7 : C_p on the airfoil surface (⊕ from [HOL 87])*

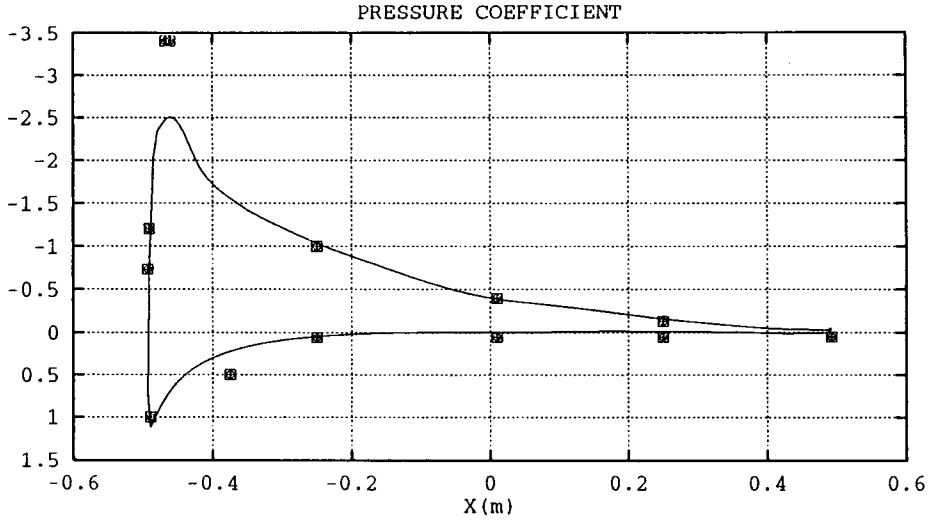

Figure 7. *Flow past a NACA 0012 at Mach 0.55 : C_p on the airfoil surface (⊕ from [HOL 87])*

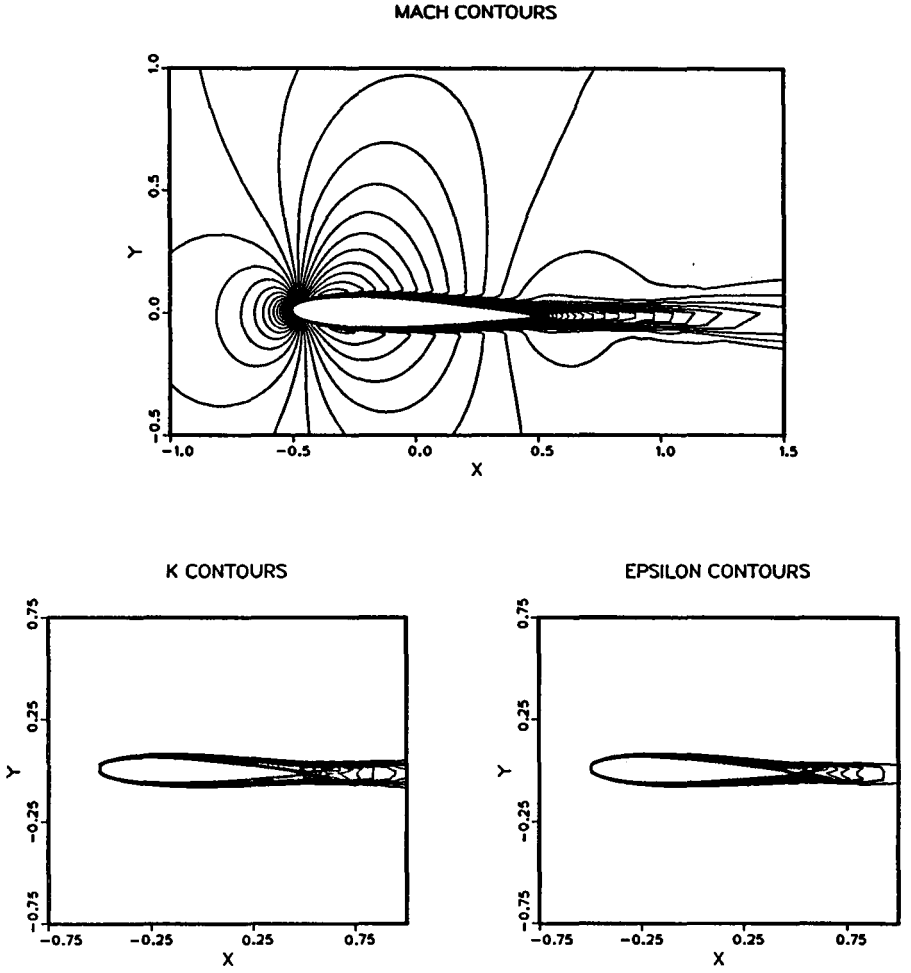

Figure 8. *Flow past a NACA 0012 at Mach 0.7 : Mach number, k and ε contours*

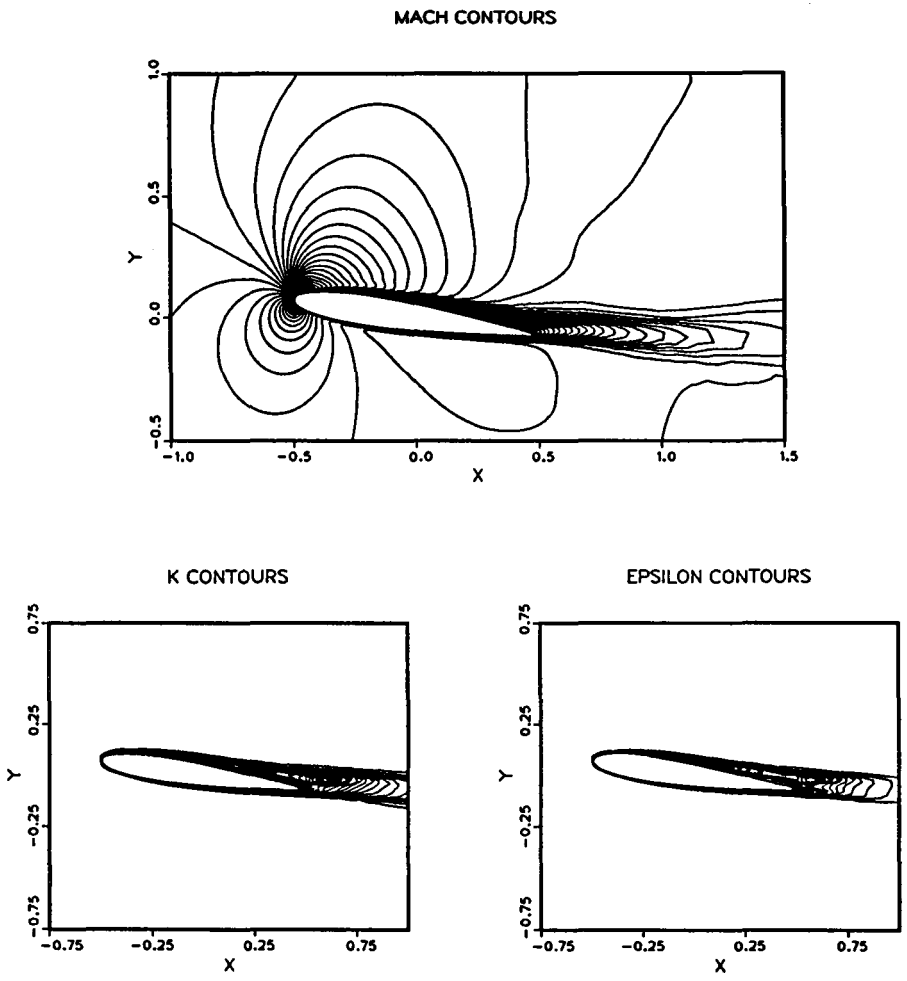

Figure 9. *Flow past a NACA 0012 at Mach 0.55 : Mach number, k and ε contours*

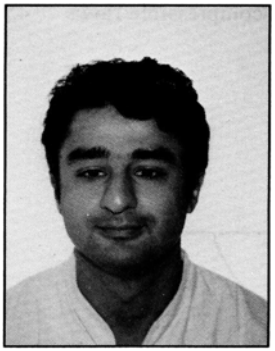

Bijan Mohammadi
Research associate at INRIA.
Post-doc at AHPCRC Minneapolis.
PH. D. Thesis, University of Paris VI in 1989.